

Specific Features of Deformation of Ni–Fe–Ga–Co Single Crystals Grown from Melt by the Stepanov Method

G. A. Malygin^a, B. I. Levandovskii^b, R. B. Timashov^a, V. M. Krymov^a, and V. I. Nikolaev^{a*}

^a Ioffe Physical Technical Institute, Russian Academy of Sciences, St. Petersburg, 194021 Russia

^b Khujand Politechnical Institute, Osimi Tajik Technical University, Khujand, 735700 Tajikistan

*e-mail: nikolaev.v@mail.ioffe.ru

Received March 19, 2020; revised March 19, 2020; accepted April 2, 2020

Abstract—The influence of thermomechanical cycles (compression along the [011] direction and recovery of the shape memory strain upon crystal heating) on the form and characteristics of the compression diagrams of Ni₄₉Fe₁₈Ga₂₇Co₆ alloy crystals not subjected to high-temperature annealing and quenching in water after the growth has been investigated. It is found that these characteristics change during the first nine cycles. Starting from the tenth thermomechanical cycle, they become stable and the deformation properties of the crystals become similar to those of quenched crystals of this alloy. This means that antiphase nanodomains are dispersed by dislocations during the thermomechanical cycling, as a result of which the disordered *B*₂ crystal structure is transformed into the ordered *L*₂₁ structure, which is characteristic of quenched crystals.

Keywords: crystal compression diagram, shape memory strain, ordered and disordered alloy structures.

DOI: 10.1134/S1063785020070202

The following specific features of deformation of Ni₄₉Fe₁₈Ga₂₇Co₆ alloy crystals quenched after annealing at temperatures of 1300–1400 K are known: diagrams of their compression in the [011] direction contain two falloffs of the flow stress, and recovery of the shape-memory (SM) strain has a burst character [1, 2]. Quenched crystals exhibit stable deformation behavior during thermomechanical cycles of compression and SM strain recovery upon heating of a deformed sample [1]. The compression diagrams of the unquenched crystals contain only one flow-stress falloff, which starts at a stress value that is twice as large as that of the first falloff in the compression diagram of the quenched sample. The SM strain recovery in the unquenched samples occurs smoothly, and its temperature range widens with an increase in the number of thermomechanical cycles [1].

The purpose of this Letter was to reveal specific features of the deformation behavior of Ni₄₉Fe₁₈Ga₂₇Co₆ alloy crystals that were not quenched after the growth. It is also of interest to analyze the stability of their properties at thermomechanical cycles of compression and heating of the strained samples. In comparison with our previous study [1], the number of compression–heating cycles is increased from 5 to 15, which made it possible to reveal previously unnoted features of the deformation behavior of the crystals under consideration. The experiments on compression along the [011] direction were carried out at a temperature of 293 K for 3.6-mm-high polished samples with a cross

section of 1.7 × 2 mm spark-cut from single-crystal preforms grown by the Stepanov method. At cutting, the crystals were oriented by the X-ray method so that their long faces corresponded to the [011] direction, in which the samples were uniaxially compressed. In all the compression cycles, the set SM strain corresponded to the total transformation strain of ~5%.

Figure 1 shows 2 of 15 compression diagrams of the alloy crystals under study. These compression diagrams are related to the 1st (curve 1) and 13th (curve 2) thermomechanical cycles. It is noteworthy that both diagrams contain only one flow-stress falloff and the stress value in the 1st thermomechanical cycle is about twice as high as that in the 13th cycle. Figure 2 shows the dependences of the stress values corresponding to the maximum (curve 1) and minimum (curve 2) in the compression diagrams on the number of thermomechanical cycles *N*. One can see that the deformation behavior of the Ni–Fe–Ga–Co alloy crystals during thermomechanical compression–heating cycles is stabilized beginning with the ninth cycle. In contrast to the large spread of stresses σ_1 and σ_2 in the first eight cycles, their values in the subsequent cycles are stabilized and become independent of the cycle number. At the same time, as was shown experimentally, the SM strain recovery acquires a pronounced burst character beginning with the tenth cycle, which was previously assumed to be typical of only crystals of this alloy quenched at high temperatures.

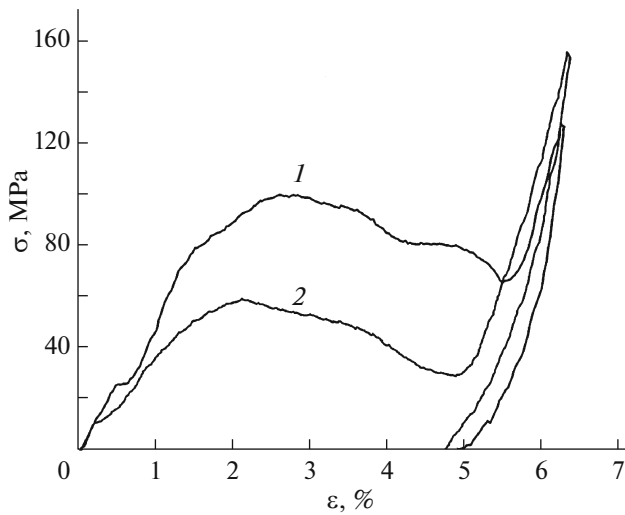


Fig. 1. Diagrams of compression along the [011] direction of the $\text{Ni}_{49}\text{Fe}_{18}\text{Ga}_{27}\text{Co}_6$ alloy crystals that were not subjected to high-temperature annealing after the (1) 1st and (2) 13th thermomechanical cycles of compression and SM-strain recovery.

This effect was not observed in [1] because of the smaller number of tests: in the first cycle, the unquenched crystal exhibited step SM strain recovery, while all the subsequent compression–heating cycles were accompanied by smooth recovery of this strain (the recovery temperature range became wider with each new cycle). This result was explained by the fact that the martensitic deformation onset stress for the unquenched crystals is much higher than that of the quenched crystals [1]. Therefore, lattice defects (dislocations) may be formed in the unquenched crystals, which may cause partial relaxation of the interface (martensite–austenite) stress. This relaxation reduces the interface stress below the critical value required for the step SM strain recovery onset [2].

The interface stresses observed in this study and their dependences on the number of thermomechanical cycles can be estimated based on the difference between the stresses corresponding to the maximum and minimum values in the compression diagrams (Fig. 2). Their difference $\Delta\sigma = \sigma_1 - \sigma_2$ is shown in Fig. 3. One can observe a large spread in the interface stresses in first several thermomechanical cycles; however, the stresses are stabilized beginning with the tenth cycle and show a tendency to decrease with a further increase in the number of cycles.

Thus, the new data on the deformation behavior upon compression and SM strain recovery in Ni–Fe–Ga–Co alloy crystals that were not quenched after the growth supplement the previously obtained data [1]. The combination of these data poses the following questions. Why is the martensitic-deformation onset stress for unquenched crystals much higher than that for the quenched ones? Why do these stresses decrease

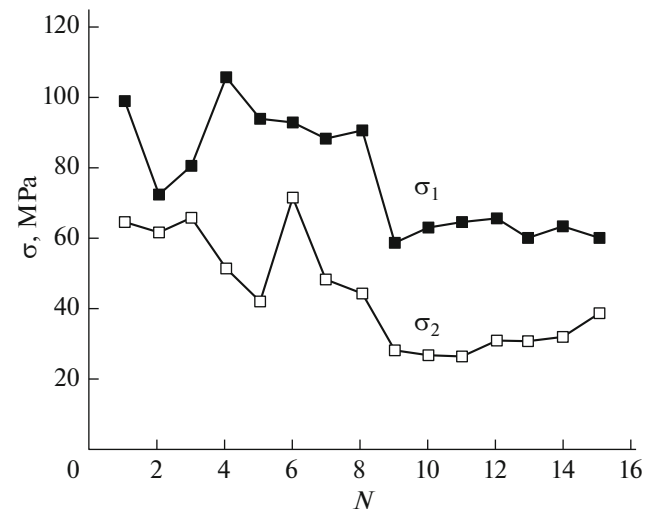


Fig. 2. Dependences of the stresses corresponding to the (1) maximum σ_1 and (2) minimum σ_2 in the compression diagrams of the $\text{Ni}_{49}\text{Fe}_{18}\text{Ga}_{27}\text{Co}_6$ alloy crystals (Fig. 1) on number N of thermomechanical cycles.

during thermomechanical cycles to the level characteristic of the quenched crystals? Finally, why, after the tenth thermomechanical cycle, is the deformation behavior of the unquenched crystal stabilized, and why does the SM strain recovery acquire a burst character (as in the quenched crystal) at temperatures of 308–328 K? In this study, we discuss these questions only from the qualitative point of view, using the data in the literature on the structures of the considered alloy and similar alloys [3–5].

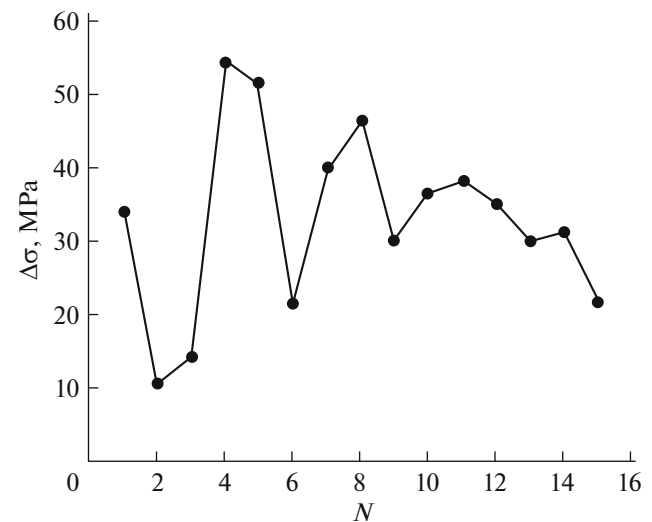


Fig. 3. Difference between the stresses $\Delta\sigma = \sigma_1 - \sigma_2$ corresponding to the maximum and minimum in the compression diagrams of the $\text{Ni}_{49}\text{Fe}_{18}\text{Ga}_{27}\text{Co}_6$ alloy crystals (Fig. 2) in dependence on the number of thermomechanical cycles.

A characteristic feature of crystals of some alloys (e.g., Co–Ti [3], Ni–Fe–Ga [4], and Ni–Fe–Ga–Co [5]) that have not been annealed at high temperature is a disordered B_2 structure containing (according to electron microscopy data [3]) dispersed antiphase domains 10–40 nm in size. Their presence increases the martensitic-deformation onset stress of an unquenched crystal. This stress significantly decreases upon crystal annealing at temperatures above 1000 K [3], and the crystal structure after the high-temperature annealing and quenching corresponds to the ordered $L2_1$ structure. Under stress, it is transformed into a twinned $14M/10M$ structure or detwinned $L1_0$ martensitic structure. Therefore, one can reasonably suggest that, in our case, the Ni–Fe–Ga–Co alloy crystal that was not annealed after the growth underwent a gradual transition from the disordered B_2 structure to the ordered $L2_1$ structure during mechanical compression cycles. Since the onset stress of the crystal martensitic deformation is almost two times lower in this case (Fig. 1), one can reasonably suggest that the crystal-compression cycles facilitate the dispersion of antiphase domains by repeatedly cutting them with slip dislocations. As a result, after ten thermomechanical cycles, the B_2 crystal structure is transformed into an $L2_1$ structure, which is the same as for the quenched crystal and possesses all its deformation properties: stability under cyclic strain and (in the presence of interface stress) a stable burst character of the SM strain recovery. The presence of one flow-stress falloff in the compression diagrams of the crystals with both B_2 and $L2_1$ structures indicates a single-stage ($B_2/L2_1 \rightarrow L1_0$) character of martensitic transitions in the alloy, which is also confirmed by the calorimetric analysis of the crystal with the B_2 structure [6].

Thus, it was shown for the first time that, in regard to the loading diagrams and strain-recovery kinetics, the cyclic thermomechanical effect on the as-grown $\text{Ni}_{49}\text{Fe}_{18}\text{Ga}_{27}\text{Co}_6$ crystals is aging of the sample. The result of this aging is similar to that of conventional heat treatment (high-temperature annealing and quenching in water) of these crystals after the growth.

CONFLICT OF INTEREST

The authors declare that they have no conflict of interest.

REFERENCES

1. G. A. Malygin, V. I. Nikolaev, B. M. Krymov, and A. V. Soldatov, *Tech. Phys. Lett.* **46**, 260 (2020). <https://doi.org/10.1134/S106378502003027X>
2. G. A. Malygin, V. I. Nikolaev, B. M. Krymov, S. A. Pul'nev, and S. I. Stepanov, *Tech. Phys.* **64**, 819 (2019). <https://doi.org/10.1134/S1063784219060124>
3. H. Kawaia, H. Kaneno, M. Yoshida, and T. Takasugi, *Intermetallics* **11**, 467 (2003). [https://doi.org/10.1016/S0966-9795\(03\)00026-8](https://doi.org/10.1016/S0966-9795(03)00026-8)
4. T. Omori, N. Kamiya, Y. Sutou, K. Oikawa, R. Kainuma, and K. Ishida, *Mater. Sci. Eng., A* **378**, 403 (2004). <https://doi.org/10.1016/j.msea.2003.10.366>
5. E. E. Timofeeva, E. Yu. Panchenko, N. G. Vetoshkina, Yu. I. Chumlyakov, A. I. Tagiltsev, A. S. Eftifeeva, and H. Maier, *Rus. Phys. J.* **59**, 1251 (2016). <https://doi.org/10.1007/s11182-016-0899-0>
6. V. I. Nikolaev, S. I. Stepanov, P. N. Yakushev, V. M. Krymov, and S. B. Kustov, *Intermetallics* **119**, 106709 (2020). <https://doi.org/10.1016/j.intermet.2020.106709>

Translated by A. Sin'kov